High Temperature Superconductor Cables in the German High Voltage Grid

Leonard Kluss, Gerrit Schlömer, Lutz Hofmann
Leibniz University of Hannover
Institute for Electrical Power Systems
Hannover, Germany
kluss@ stud.uni-Hannover.de

***Abstract*— This paper describes high temperature superconducting (HTS) cable characteristics and their impact on the German high voltage transmission grid. The characteristics are the result of computed cable construction properties. They are calculated for every possible design of each HTS layer and their combination, if multiple layers are necessary. The final cable design is chosen by its alternating current losses or respectively its current distribution.**

The influence of HTS cables on the German high voltage transmission grid is shown for eight different cases. This case study replaces planned cable sections stepwise by HTS cables.

I. INTRODUCTION

In 1908 the research of H. Kamerlingh Onnes lead to liquefied helium and enabled his discovery of a zero resistance conductor at approximately 4 K in 1911 [1]. Seventy-five years after discovering the first superconductor J. G. Bednorz and K. A. Müller found a ceramic compound with a critical temperature of 77 K [2]. Due to the decrease in cooling efforts for those high temperature superconductors new possibilities of economic use especially in the electric power system were created.

Today the use of superconducting cables is a promising opportunity of creating a transmission line with low energy losses, no requirement of large route widths, nearly no temperature influence and negligible outer magnetic fields, while enabling a high energy transport. The development of superconducting cables already led to the construction of a 275 kV-3 kA cable [3] [4], which still creates a gap to the high voltage level in Germany. Furthermore the rapid development of second generation HTS wire with rising critical current I_C, led to a world record of 228 A per 4 mm wide HTS wire [5]. Due to this progress and advantages, distribution and transmission operators take this technology into account [6][7][8].

This paper presents the analyses of the influence of this technology on the German high voltage grid by replacing parts of the planned 380 kV transmission line between Ganderkesee and St. Hülfe with HTS cable sections. The parameters of the cable used for the simulations are calculated using a newly developed algorithm that computes possible HTS cable designs. As input parameters the algorithm uses the voltage level, the HTS wire type data and the required transmission capacity. Additionally temperature and position of the dielectrics in regard to the cryostat are needed as input since they have a strong influence on the cable design and parameters.

II. HTS CABLE PROPERTIES

The properties of HTS cable depend on different construction options of which only coaxial cables are contemplated.

A. Cable Construction

HTS cables for high voltage transmission purposes can mainly be classified into two different categories by their dielectrics position. Constructions with cold dielectrics (CD) maintain a temperature gradient between coat and other cable components, while in warm dielectric models the insulation and conductor layers are separated by the cryostat. Consequently insulation, shield layers and coating remain at ambient temperature [9]. Due to advantages of CD HTS cables this construction type is chosen. The cable construction from its core to the outer radius starts with a former as the base for conductor layers. A layer is wrapped with carbon paper and consists of YBCO, a second generation HTS. On this base a poly-propylene laminated paper (PPLP) insulation is wrapped around the conductors and is followed by shield layers. This electrical part of the cable is surrounded by a protection layer and a cryostat, as thermal insulation [10].

B. HTS Layer Design

The design of a HTS layer is shown in Fig. 1, where *r* represents the radius, *W* the cross sections wire width and *w* the actual wire width of the layer. Including the gap *g* between two conductors of one layer and the distribution angle τ, the correlation given in (1) arises.

$$r \cdot \tan\left(0.5 \cdot \tau\right) = \frac{g}{2} \cdot \frac{1}{\cos\left(0.5 \cdot \tau\right)} + \frac{W}{2} \tag{1}$$

Furthermore the pitch l_p, which will serve as variable for the inductance calculation, can be determined by (2), using the winding angle θ.

$$l_p = 2\pi r \cdot \left(\tan\left(\theta\right)\right)^{-1} \tag{2}$$

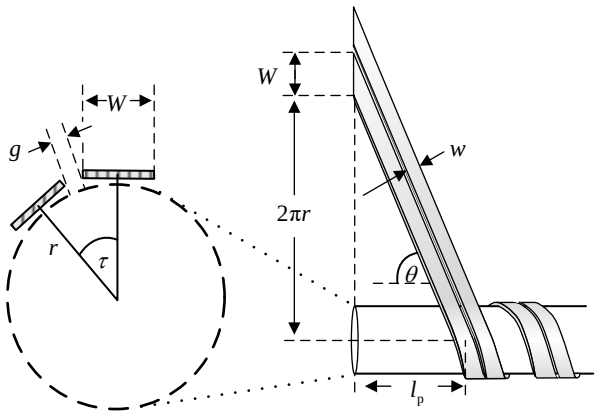

Figure 1. Cross section and side view of a HTS layer [10]

The gap size can be seen as a constant distance, but it has to fulfill the criteria given in (3), which includes the free contract rate ε_t and the number of used wires d [11].

$$g \geq \frac{\varepsilon_t}{d} \cdot 2\pi r \left(1 + \left(\frac{l_p}{2\pi r} \right)^2 \right) \tag{3}$$

The minimum total number of HTS tapes d_t can be determined using the critical current I_C, the rated current I_0 and the margin η, shown in (4) [10]. Taking (1), (2) and (3) in account, d_t determines the number of layers.

$$d_t \geq \frac{\sqrt{2} I_0}{I_C} (1 + \eta) \tag{3}$$

III. CABLE CHARACTERISTICS

A. Resistance

Since the characteristic of a zero resistance material can only be fulfilled for direct currents, AC losses need to be included. Equation (2) describes the hysteresis loss of a HTS wire, which will serve as approximation of the AC losses per length $P'_{AC,i}$. These losses depend on the frequency f, the critical current I_C and the current proportion factor F_i of layer i, given in (5) [10][12].

$$P'_{AC,i} = \frac{I_C^2 \mu_0 f}{\pi} \left((1 - F_i) \cdot \ln(1 - F_i) + (1 + F_i) \cdot \ln(1 + F_i) - F_i^2 \right) \tag{4}$$

$$F_i = \frac{I_{i,0} \cdot \sqrt{2}}{I_C \cdot d_i} \tag{5}$$

Equation (6) indicates the resistance per length, and was determined as approximation, where n_C represents the number of conductor layers.

$$R'_{HTS} = \sum_{i=1}^{n_C} \frac{\sqrt{(2\pi r_i)^2 + I_{p,i}^2}}{l_{p,i}} \cdot \frac{d_i \cdot P'_{AC,i}}{I_{i,0}^2} \tag{6}$$

B. Inductance

The self-inductance of layer i and the coupling inductance of two layers i and j is given by (8) and (9), with the outer most radius D. The value of a factor α can either be one or minus one, depending on the winding directions of the layers, with their product being negative for different and positive for equal winding directions. Note that (8) is only valid if j is greater than i [10].

$$L_i = \frac{\mu_0 \pi r_i^2}{l_{p,i}^2} + \frac{\mu_0 \cdot \ln(D / r_i)}{2\pi} \tag{7}$$

$$M_{i,j} = \alpha_i \alpha_j \frac{\mu_0 \pi r_i^2}{l_{p,i} l_{p,j}} + \frac{\mu_0 \cdot \ln(D / r_j)}{2\pi} \tag{8}$$

Calculating self and coupling inductance for each layer and layer combination leads to (10), taking (9) into account.

$$M_{i,j} = M_{j,i} \tag{9}$$

$$\boldsymbol{M} = \left(\begin{array}{cccc:ccc} L_1 & M_{1,2} & \cdots & M_{1,n_C} & M_{1,n_C+1} & \cdots & M_{1,n} \\ M_{2,1} & L_2 & \cdots & M_{2,n_C} & M_{2,n_C+1} & \cdots & M_{2,n} \\ \vdots & \vdots & \ddots & \vdots & \vdots & \ddots & \vdots \\ M_{n_C,1} & M_{n_C,2} & \cdots & L_{n_C} & M_{n_C,n_C+1} & \cdots & M_{n_C,n} \\ \hdashline M_{n_C+1,1} & M_{n_C+1,2} & \cdots & M_{n_C+1,n_C} & L_{n_C+1} & \cdots & M_{n_C+1,n} \\ \vdots & \vdots & \ddots & \vdots & \vdots & \ddots & \vdots \\ M_{n,1} & M_{n,2} & \cdots & M_{n,n_C} & M_{n,n_C+1} & \cdots & L_n \end{array} \right) \tag{10}$$

Equation (11) serves as an approximation for the inductance of the cable model. The inclusion of the current distribution requires the preceding solution for the current of each layer and is used instead of current distribution factors for descriptiveness.

$$L'_{HTS} = \frac{1}{n_C} \left(\sum_{\substack{l=1 \\ l \neq k}}^{n_C} \sum_{k=1}^{n} I_l M_{kl} + \sum_{j=1}^{n_C} I_j L_j \right) \left(\sum_{i=1}^{n_C} I_i \right)^{-1} \tag{11}$$

C. Capacitances and Conductance

The insulation is created for all layer variations, due to its dependency of the inner radius or respectively the maximum electrical field intensity. The schematic illustration of an insulation made out of PPLP is shown in Fig. 2. Starting point for the evaluation of the maximum field intensity, the former radius and consequently the insulation design is the construction of a 275 kV HTS cable [3][13].

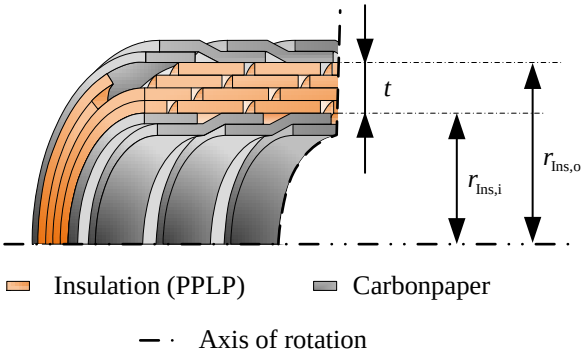

Figure 2. Polypropylene laminated paper insulation [14]

Insulation designs can be derived from known data by comparing their maximum field intensity, leading to (12) and (13). The index "sc" indicates a scaled parameter, while U_{rel} is defined as the quotient of the required and the initially voltage level.

The thickness t and the inner radius $r_{\mathrm{Ins,i,sc}}$, scaled for the required voltage level, determine the scaled outer radius $r_{\mathrm{Ins,i,sc}}$.

$$t = r_{\mathrm{Ins,i,sc}} \cdot \left(\exp\left(U_{\mathrm{rel}} \cdot \frac{r_{\mathrm{Ins,i}}}{r_{\mathrm{Ins,i,sc}}} \cdot \ln\left(\frac{r_{\mathrm{Ins,o}}}{r_{\mathrm{Ins,i}}} \right) \right) - 1 \right) \tag{12}$$

$$r_{\mathrm{Ins,o,sc}} = r_{\mathrm{Ins,i,sc}} \cdot \exp\left(U_{\mathrm{rel}} \cdot \frac{r_{\mathrm{Ins,i}}}{r_{\mathrm{Ins,i,sc}}} \cdot \ln\left(\frac{r_{\mathrm{Ins,o}}}{r_{\mathrm{Ins,i}}} \right) \right) \tag{13}$$

Note that an increasing radius leads to smaller insulation properties, due to decreasing field intensity at the inner insulation radius. Both of these effects combined show the existence of a minimum cable thickness. It can be considered as a design, considering mechanical properties like the bending radius.

The capacitance and conductance are depending on the insulation thickness. Their dependency is given by (14) and (15) with the loss factor $\tan(\delta)$. Values of $\tan(\delta)$ can be found in [14].

$$C'_{\mathrm{HTS}} = 2\pi\varepsilon_0\varepsilon_{\mathrm{r}} \cdot \ln^{-1}\left(\frac{r_{\mathrm{Ins,o}}}{r_{\mathrm{Ins,i}}} \right) \tag{14}$$

$$G'_{\mathrm{HTS}} = 2\pi\varepsilon_0\varepsilon_{\mathrm{r}}\omega \cdot \tan(\delta) \cdot \ln^{-1}\left(\frac{r_{\mathrm{Ins,o}}}{r_{\mathrm{Ins,i}}} \right) \tag{15}$$

D. Winding Angle Variations

In (6), (7) and (8) the dependency of line parameters and the winding angles is displayed. To optimize the cable construction all possible layer designs and combinations of those designs are compared. The alterations include angle variations between 12° and 32° and a change of the winding direction. Due to variation of the winding angle and therefore of HTS tapes per layer, different cable designs can show a different number of HTS layers, different thickness and insulation design. The final design is chosen by its current distributions or losses, while an equal current distribution in all conductor layers is wanted to ensure minimal losses.

IV. Results of the Cable Simulation

Table I showcases HTS cable parameters of two different designs. The model A was designed for a power transmission of 2200 MVA per three-phase system. Model B was designed for a transmission of 1100 MVA per system. Due to the algorithm used for constructing the cable, this requirement is surpassed and a layer design for higher energy transmission results. Therefore the cable has a small overload capability.

TABLE I. HTS Cable Characteristics

Characteristic	**Model**	
	A	***B***
L´	0.593 mH/km	0.4 mH/km
R´	0.288 mΩ/km	0.114 mΩ/km
C´	126.6 nF/km	124.9 nF/km
G´	39.8 nS/km	39.2 nS/km

V. Impact

To evaluate the impact of HTS cables on the German high voltage grid a simulation environment for an integrated grid and market simulation is used. The program and its data base in detail are described in [15].

The simulations are performed exemplary with variations of the 380 kV transmission line between Ganderkesee and St. Hülfe. This connection is part of the grid development plan (NEP) in Germany and will consist of four cable and three overhead transmission line sections. The partial to complete replacement of cable sections with HTS cables of type A and type B result in nine cases (C1, C2A, C2B to C5B) shown in Table II. All overhead transmission line sections, with a total length of 42.55 km, maintain their properties.

Simulation results of losses and the need of reactive power are shown in Table III. They are listed in their relation to case C1, which represents the conventional technologies. It should be noted that the displayed relations count for all cable and overhead line segments combined. Consequently the displayed results compare the planned connection between Ganderkesee and St. Hülfe with the respective case.

TABLE II. Analyzed Cases and their HTS Cable Proportion

Case	**Cable type distribution**	
	2XS(FL)2Y 1x2500 RMS/250/	***HTS A or B***
C1	18.2 km	0 km
C2	15 km	3.2 km
C3	11.2 km	6.9 km
C4	5.6 km	12.5 km
C5	0 km	18.2 km

TABLE III. REDUCTION OF POWER LOSSES AND NEED OF REACTIVE POWER BY PARTIAL TO COMPLETE REPLACEMENT OF STANDARD CABLES BY HTS CABLE TECHNOLOGY

		Case			
		C2	***C3***	***C4***	***C5***
P_V	A	89.05 %	77.40 %	60.77 %	47.49 %
	B	91.06 %	81.31 %	67.32 %	56.27 %
Q_B	A	84.52 %	67.09 %	41.31 %	16.52 %
	B	86.97 %	72.24 %	50.36 %	29.18 %

All cases show decreasing losses and less need of reactive power. This characteristic is more concise for longer HTS cable proportions. Losses can be reduced up to 47.49 %, while the demand of reactive power declines to 16.52 %. It shall be pointed out that due to different properties of the cable parts in every case, different power flows result. Furthermore the number of systems varies depending on the cable type. To enable the power transmission requirements two times the amount of systems of HTS type B are needed to replace one HTS type A system.

The difference in demand of reactive power and the changes in the power flow cause variations in node voltages. The maximum of these variations is displayed in Table IV. The data is presented as the maximum node voltage decrease in the German grid in relation to the rated node voltage, displaying the greatest influence in case C5A with 0.0296 p.u..

TABLE IV. MAXIMUM VOLTAGE DROP

Power	**Voltage drop in p.u.**			
	C2	***C3***	***C4***	***C5***
A	0.0066	0.0144	0.0231	0.0296
B	0.0054	0.0118	0.0194	0.0253

SUMMARY AND CONCLUSION

The HTS cable design is chosen by its minimum losses, as a result of winding angle variations. Due to that criterion for the cable construction, an overload capability results. This indicates an oversizing and the necessity of program expansions to fulfill power transmission requirements with more precision.

The results of the HTS cable simulation show an inductance of a similar magnitude, compared to the conventional cable type. Its resistance is below the conventional magnitude like expected, while the capacitance and conductance is about halved.

Using the calculated cable proportions for the power flow and integrated market simulation a decrease of power losses, a decreasing demand of reactive power and lower node voltages are resulting, with a higher variance for longer HTS sections.

ACKNOWLEDGMENT

The authors thank Mr. D. Kottonau of the Kalsruhe Institute of Technology (KIT) for the support and contributions.

They thank their colleagues at the Institute of Electrical Power Systems, Hannover, Germany and especially Dr. T. Rendel for support and discussions.

REFERENCES

[1] P. Kes; D. van Delft, The Discovery of Superconductivity, Physicy Today, pp. 38-43, S-0031-9228-1009-020-4, September 2010.

[2] M. Bäcker, „Funktionswerkstoffe,“ [Functunal Materials], 1st ed., Wiesbaden, 2014, pp. 237-238, in German.

[3] M. Yagi, S. Mukoyama, T. Mitsuhashi, T. Jun, J. Lui, R. Nakayama, N. Hayakawa, X. Wang, A. Ishiyama, N. Amemiya, T. Hasegawa, T. Saitoh, T. Ohkuma and O. Maruyama, “Design and evaluation of 275 kV-3 kA HTS power cable,” *Phys. Procedia*, vol. 45, pp. 277-280, 2013.

[4] M. Yagi, S. Mukoyama, N. Amemiya, A. Ishiyama, X. Wang, Y. Aoki, T. Saito, T. Ohkuma and O. Maruyama, ”Progress of 275 kV–3 kA YBCO HTS cable,” *Physica C*, vol. 471, Issues 21-22, pp. 1274-1278, 2011.

[5] Y. Iijima, “High-performance Y-based superconducting wire and their applications,” 2013

[6] M. Stemmle, F. Merschel, M. Noe and A. Hobl, “AmpaCity – Advanced superconducting medium voltage system for urban area power supply,” in *Proc. IEEE PEST T&D Conf. Expo.*, 2014, pp. 1-5.

[7] J. Isles, A Superconducting ‘SuperStation’, *The Energy Industry Times*, November 2010, pp.15.

[8] TenneT Holding B. V., HTS Cable, 2016.
Online source: http://www.tennet.eu/our-key-tasks/innovations/hts-cable/

[9] H. Okubo, M. Noé, J. Cho and A. Wolsky, “Status of development and field test experience with hight-temperature superconducting power equipment,” Cigré Working Group D1.15, Paris, France, Tech. Rep. 418, Jun. 2010

[10] Y. Wang, Fundamental Elements of Applied Superconductivity in Electrical Engineering, Science Press: ISBN: 978-1-118-45114-4, 2013.

[11] Y. Wang, F. Zhang, Z. Gao, Z. Zhu, S. Dai, L. Lin and L. Xiao „Development of a high-temperature superconducting bus conductor with large current capacity,” *Supercond. Sci.. Technol.*, vol. 22, no. 5, May 2009.

[12] D. Kottonau, E. Shabagin, M. Noe and S. Grohmann, “Opportunities for high-voltage AC superconducting cables as part of new long-distance transmission lines,” *IEEE Transactions On Applied Superconductivity*, vol. 27, Issue 4, 2017.

[13] M. Yagi, J. Lui, S. Mukoyama, T. Mitsuhashi, J. Teng, N. Hayakawa, X. Wang, A. Ishiyama, N. Amemiya, T. Hasegawa, T. Saitoh, O. Maruyama and T. Ohkuma, “Experimental results of 275-kV 3-kA REBCO HTS power cable,” *IEEE Transactions On Applied Superconductivity*, vol. 25, Issue 3, 2015.

[14] T. Takahashi, H. Suzuki, M. Ichikawa, T. Okamoto, S. Akita, S. Maruyama and A. Kimura, “Dielectric properties of 500 m long HTS power cable,” *IEEE Transactions On Applied Superconductivity*, vol. 15, Issue 2, 2005.

[15] T. Rendel, „Erweiterung und Plausibilisierung eines Modells für die integrierte Simulation des europäischen Verbundnetzes und Strommarktes,“ [Extension and Verification of a Model for an Integrated Simulation of the European High Voltage Grid and Energy Market], 2015, in German.